



# An experimental water line list at 1950 K in the 6250–6670 cm<sup>-1</sup> region



Lucile Rutkowski<sup>a</sup>, Aleksandra Foltynowicz<sup>a</sup>, Florian M. Schmidt<sup>b</sup>, Alexandra C. Johansson<sup>a</sup>, Amir Khodabakhsh<sup>a</sup>, Aleksandra A. Kyuberis<sup>c</sup>, Nikolai F. Zobov<sup>c</sup>, Oleg L. Polyansky<sup>d</sup>, Sergei N. Yurchenko<sup>d</sup>, Jonathan Tennyson<sup>d,\*</sup>

<sup>a</sup> Department of Physics, Umeå University, 901 87 Umeå, Sweden

<sup>b</sup> Thermochemical Energy Conversion Laboratory, Department of Applied Physics and Electronics, Umeå University, 901 87 Umeå, Sweden

<sup>c</sup> Institute of Applied Physics, Russian Academy of Sciences, Ulyanov Street 46, Nizhny Novgorod, Russia 603950, Russia

<sup>d</sup> Department of Physics and Astronomy, University College London, London, WC1E 6BT, UK

## ARTICLE INFO

### Article history:

Received 29 August 2017

Revised 25 October 2017

Accepted 25 October 2017

Available online 27 October 2017

### Keywords:

Water

Absorption

Fourier transform spectroscopy

Optical cavity

Frequency comb

*ab initio* Calculations

## ABSTRACT

An absorption spectrum of H<sub>2</sub><sup>16</sup>O at 1950 K is recorded in a premixed methane/air flat flame using a cavity-enhanced optical frequency comb-based Fourier transform spectrometer. 2417 absorption lines are identified in the 6250–6670 cm<sup>-1</sup> region with an accuracy of about 0.01 cm<sup>-1</sup>. Absolute line intensities are retrieved using temperature and concentration values obtained by tunable diode laser absorption spectroscopy. Line assignments are made using a combination of empirically known energy levels and predictions from the new POKAZATEL variational line list. 2030 of the observed lines are assigned to 2937 transitions, once blends are taken into account. 126 new energy levels of H<sub>2</sub><sup>16</sup>O are identified. The assigned transitions belong to 136 bands and span rotational states up to J = 27.

© 2017 The Authors. Published by Elsevier Ltd.

This is an open access article under the CC BY license. (<http://creativecommons.org/licenses/by/4.0/>)

## 1. Introduction

Water is ubiquitous and its spectrum is important for a whole range of terrestrial and astronomical applications. Serious attempts have been made to characterize the spectrum of hot water both experimentally by observation of spectra [1–17] and theoretically by the computation of extensive line lists [18–24]. These line lists are used to inform databases concerned with models of hot bodies such as HITEMP [25] and ExoMol [26,27]. A comprehensive assessment of water spectroscopy was undertaken by an IUPAC task group [28,29] whose work is currently being updated [30].

The ubiquity of water means that understanding its spectrum at all wavelengths and temperatures is always important. The spectrum of hot water is of particular interest in regions where absorption by room temperature water is weak. The present work concentrates on one such region as it probes the spectrum of hot water in the conventional telecom window (1.53–1.565 μm) as well as the astronomers' H-band (1.5–1.8 μm). These regions are useful for remote sensing of hot water spectra due to the reduced atmo-

spheric absorption. Previous high-temperature water spectra analyzed for this region [10,12,13,31–35] were recorded in emission in flames at atmospheric pressure at moderate spectral resolution; in addition, due to the lack of thermal stability, these spectra did not provide usable information on the line intensities.

This paper presents a high temperature water absorption spectrum measured at Umeå University. The spectrum is measured in a premixed methane/air flat flame at atmospheric pressure using a cavity-enhanced optical frequency comb-based Fourier transform spectrometer (FTS) [36]. The combination of an FTS with a frequency comb allows the measurement of broadband and high resolution molecular spectra in short acquisition times and without visible influence of the instrumental line shape [37,38], while the cavity provides high sensitivity to absorption [39]. The ability to measure the present spectrum simultaneously over a broad bandwidth reduces systematic errors and the influence of fluctuations of the environmental conditions. The spectrum is recorded at high resolution (0.033 cm<sup>-1</sup>) in the near-infrared 6250–6670 cm<sup>-1</sup> region, and line positions are identified with an accuracy of 0.01 cm<sup>-1</sup>. Knowledge of the temperature and water concentration, which have previously been measured for that specific burner by Qu et al. [40] using tunable diode laser absorption spectroscopy, as

\* Corresponding author.

E-mail address: [j.tennyson@ucl.ac.uk](mailto:j.tennyson@ucl.ac.uk) (J. Tennyson).

well as the thermally stable conditions, allow absolute line intensities to be determined.

The measured absorption spectrum is compared to the newly computed POKAZATEL hot line list [24] augmented by the inclusion of empirical energy levels [28]. This comparison allows us to assess both the contents of the measured spectrum and the reliability of the computed line list. The POKAZATEL line list is then used to make assignments to the spectrum resulting in a significant number of newly identified transitions and energy levels.

The following two sections of the paper describe the experimental set-up and results. Section 4 presents the experimental water line list. Comparisons with the computed line lists, particularly the most recent one [24], are given in Section 5, followed by conclusions in Section 6.

## 2. Experimental setup

The experimental setup is described in detail in references [36,41] and is therefore only briefly summarized here. The spectrometer consists of an Er:fiber femtosecond laser with a repetition rate of 250 MHz ( $0.0083\text{ cm}^{-1}$ ), a 60 cm long enhancement cavity with a finesse of around 150, and a fast-scanning Fourier transform spectrometer (FTS). The comb is locked to the cavity using the two-point Pound-Drever-Hall method [39,42] with locking points at 6330 and  $6450\text{ cm}^{-1}$ . The cavity is open to air, and a flat flame burner [43] is placed in its center. The burner is operated on premixed methane/air at stoichiometric ratio with a total flow rate of 10 L/min. The comb beam probes the line of sight in the flame (flame diameter of 3.8 cm) at atmospheric pressure and at a height above the burner (HAB) of 2.5 mm. At this HAB the temperature and species are rather homogeneously distributed along the line of sight [40,43], the average flame temperature is  $1950 \pm 50$  K, the average water concentration is  $17 \pm 1\%$  (both characterized using tunable diode laser absorption spectroscopy [40]), and the average hydroxide (OH) concentration is 0.28% [41].

The light transmitted through the cavity is coupled into an optical fiber connected to the input of a fast-scanning FTS with an auto-balancing detector that acquires a spectrum with  $0.033\text{ cm}^{-1}$  resolution in 0.4 s. The optical path difference is calibrated using a stabilized HeNe laser whose beam is co-propagating with the comb beam in the FTS. The wavelength of the HeNe laser is calibrated by comparing the positions of the OH lines in the spectrum to the line positions in the 2012 edition of the HITRAN database [44]. The standard deviation of the relative difference between the experimental and HITRAN OH line positions is  $0.0076\text{ cm}^{-1}$ . Since HITRAN does not contain data on the pressure shift of the OH lines, we estimate the shift to be 10% of the pressure broadening at atmospheric pressure, i.e.  $0.007\text{ cm}^{-1}$ . Thus we estimate that the frequency accuracy of the spectrum is  $0.01\text{ cm}^{-1}$ . The high-temperature spectrum is averaged 20 times and normalized to a background spectrum measured when the flame is off. The baseline is additionally corrected for slowly varying etalons fringes.

We note that the influence of broadband flame emission can be neglected since the probability of emission into the cavity mode is low and the cavity thus acts as an effective filter. Moreover, the collimator for coupling the cavity transmitted light into the fiber does not face the flame and is placed few tens of cm away from the flame, where the intensity of emission is already very low.

## 3. Cavity-enhanced absorption spectrum

The normalized transmission spectrum measured in the flame is shown in Fig. 1(a). To extract the absorption coefficient from this spectrum, we use the model for the normalized transmission,  $I_T$ ,

given by Foltynowicz et al. [42]

$$I_T(\nu) = \frac{(1-r)^2 \exp[-\alpha(\nu)L]}{1 + r^2 \exp[-2\alpha(\nu)L] - 2r \exp[-\alpha(\nu)L] \cos[2\phi(\nu)L + \varphi(\nu)]}, \quad (1)$$

where  $L$  is the interaction length between the light and the sample (i.e. the flame diameter),  $r$  is the frequency-dependent intensity reflection coefficient of the cavity mirrors, determined experimentally by cavity ringdown,  $\alpha$  and  $\phi$  are the molecular absorption and dispersion coefficients, respectively, and  $\varphi$  is the round-trip phase shift in the cavity. The round-trip intracavity phase shift is equal to a multiple of  $2\pi$  for comb lines locked to the centers of the corresponding cavity modes. Because of the intracavity dispersion, caused by the cavity mirror coatings as well as the gas sample inside the cavity, the cavity modes are not equally spaced and only the comb lines around the locking points are exactly on resonance with their corresponding cavity modes [42]. However, because of the low cavity finesse, the relative comb-cavity offset is small in the entire spectral range of the comb, and the intracavity phase shift can be set to  $2\pi$ , or zero. To extract the absorption coefficient from Eq. (1) we also neglect the molecular dispersion, since then the equation can be solved analytically. This approximation gives correct values for on-resonance absorption coefficients, since molecular dispersion is equal to zero at these frequencies.

The absorption spectrum obtained using the analytical solution to Eq. (1) with molecular and cavity dispersion put to zero is plotted in Fig. 1(b). The noise on the baseline is  $5 \times 10^{-7}\text{ cm}^{-1}$ , which translates into a signal-to-noise ratio (SNR) of 2400 for the strongest lines. The negative absorption values and the slight line asymmetry at frequencies above  $6550\text{ cm}^{-1}$  are caused by the neglected comb-cavity offset, which increases away from the locking points [42].

## 4. Experimental water line list

The center frequencies of absorption lines are found by taking the first derivative of the absorption spectrum [Fig. 1(b)] and finding the points where it crosses zero. Most of the absorption lines are water transitions but the spectrum contains also several OH transitions [41]. The OH transition frequencies, identified using the 2012 edition of the HITRAN database [44], as well as water lines less than  $0.02\text{ cm}^{-1}$  away from an OH line, are removed from the list. The precision of the center frequencies is below  $0.0005\text{ cm}^{-1}$  for most lines, limited by the line width of the molecular lines ( $0.7\text{ cm}^{-1}$ ) and the SNR of up to 2400. The accuracy is limited to  $0.01\text{ cm}^{-1}$  by the HeNe wavelength calibration. It should be emphasized that positions of overlapping water lines, i.e. those separated by less than the line width, cannot be identified using this method. Note also that the transition frequencies are at atmospheric pressure.

The experimental line intensities,  $S$ , are calculated from the value of absorption  $\alpha_{\max}$  corresponding to each center frequency, using

$$S = \frac{\alpha_{\max}}{n_T \chi_{\max}}, \quad (2)$$

where  $\chi_{\max}$  is the peak (on-resonance) value of the Voigt profile (in cm), and  $n_T$  is water density at the temperature  $T$  (equal to  $6.4 \times 10^{17}\text{ molecule/cm}^3$  for  $T = 1950$  K and  $[\text{H}_2\text{O}] = 17\%$ ). Since no data exists for the pressure broadening parameter of water at these temperatures, we assume a Lorentzian half width of  $0.027\text{ cm}^{-1}$  for all lines, as it matches relatively well to the data. The Doppler half width varies from  $0.0237$  to  $0.0253\text{ cm}^{-1}$  across the spectrum. The experimental line list contains 2417 lines; it is plotted in Fig. 2 and given in the supplementary information. The lowest line intensity that can be identified is  $10^{-25}\text{ cm/molecule}$ , limited by

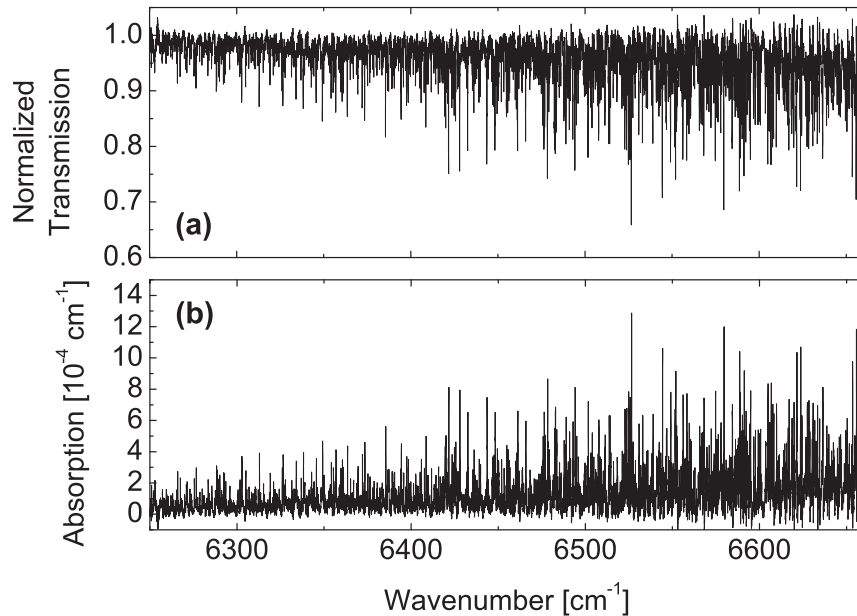


**Fig. 1.** (a) Normalized cavity-enhanced transmission spectrum in the flame at atmospheric pressure,  $[H_2O] = 17\%$  and  $T = 1950\text{ K}$ . (b) The corresponding absorption spectrum.

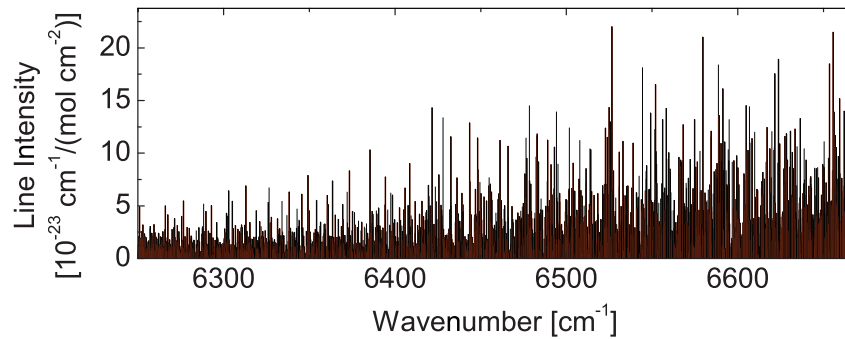


**Fig. 2.** Line intensities of water transitions at 1950 K retrieved from the measurement in the flame.

SNR in the spectrum. The uncertainty in the intensity is 6% for the strongest lines, limited mainly by the uncertainty in the water concentration, and increases for weaker lines because of the lower SNR.

To illustrate the accuracy of the experimental line list, Fig. 3(a) shows a comparison between the experimental transmission spectrum (black) and a spectrum simulated using Eq. (1) with the experimental line list, Voigt profiles with a Lorentzian half width of  $0.027\text{ cm}^{-1}$  and the intracavity round-trip phase shift put to zero (red). The difference between the measurement and the model is plotted in blue (vertically offset for clarity). The green vertical lines mark the positions of OH lines. Fig. 3(b) shows a zoom of the spectrum around one of the locking points, i.e. where the comb-cavity offset is zero. The structure in the residuum at the frequencies marked in green comes from the OH lines that are removed from the line list. The discrepancies visible at other frequencies are caused mainly by an incorrect Lorentzian width and by the remaining water lines that could not be taken into account in the line list because of their strong overlap with other lines. The amplitude of the residual increases for higher wavenumbers since the comb-cavity offset increases away from the locking points.

## 5. Line assignment

The spectral analysis of the experimental line list was performed using the recently computed POKAZATEL hot line list

[24] with energies replaced by empirical energy levels [28]. These empirical levels come from the recent IUPAC-sponsored study of water spectra [29] in which the MARVEL (measured active vibration-rotation energy levels) [45,46] procedure was used to invert measured line frequencies to obtain empirical energy levels; below, this line list is referred to as MARVEL-POKAZATEL. Using the MARVEL-POKAZATEL line list to generate a water absorption spectrum at 1950 K in the experimental wavelength range leads to about 20,000 lines with intensities between  $10^{-22}$  and  $10^{-25}\text{ cm/molecule}$ , which corresponds to the experimental intensity range.

The first step in the spectral analysis involved making a so-called trivial assignment, that is identifying lines for which both upper and lower state energy levels as well as frequencies are already known empirically. We assumed a match between MARVEL and experimental frequencies if they differ by less than about  $0.03\text{ cm}^{-1}$ , which reflects the average line width at atmospheric pressure of about  $0.07\text{ cm}^{-1}$  and the accuracy of hot MARVEL levels which is about  $0.02\text{ cm}^{-1}$ . About 1900 lines were trivially assigned by this method with about half of them being identified as blends, that is two or more MARVEL transitions associated with one experimental line.

The second step in the spectral analysis was assignment of the remaining stronger lines that were not trivially using the POKAZATEL line list. The trivially-assigned lines were also considered to be unassigned during this second step if their calculated inten-

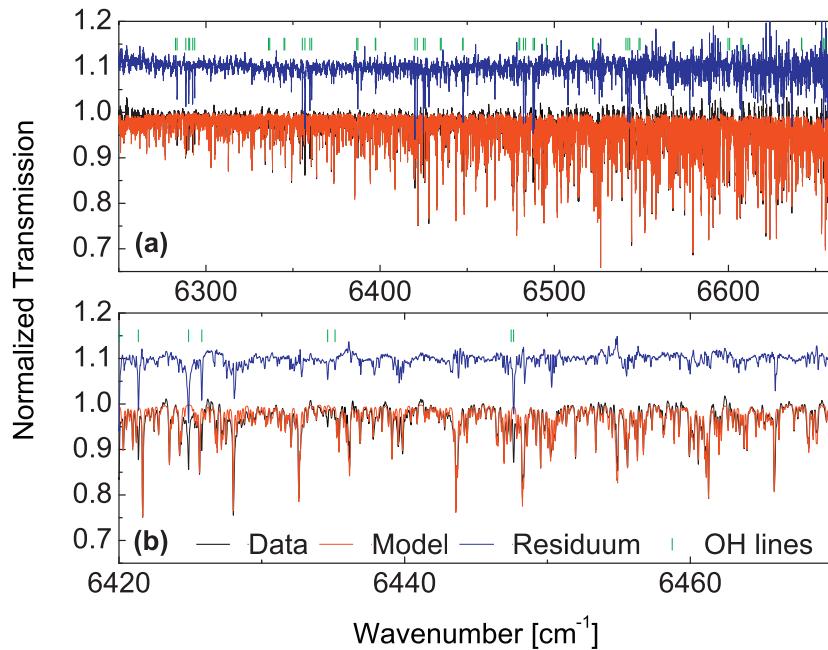


**Fig. 3.** Comparison between the measurement (black) and the spectrum calculated using the experimental line list (red). Residuum is shown in blue, vertically offset for clarity. The frequencies of the strongest OH transitions are marked by green lines. (a) Full range. (b) Enlarged section showing the general good agreement between the data and the model. (For interpretation of the references to colour in this figure legend, the reader is referred to the web version of this article.)

sity was less than half of the measured one. We only considered stronger theoretical lines with calculated intensities higher than  $10^{-23}$  cm/molecule. We concentrated on identifying those transitions which involved upper levels with quantum numbers close to MARVEL levels. This allowed us to estimate the expected observed minus calculated residue for the upper level using the difference between known MARVEL levels and levels predicted by the original POKAZATEL line list. This method of tracking states with nearby quantum numbers is sometimes known as the method of branches [4,47]; it works best for the relatively rare, stronger experimental lines. Use of this method led to the assignment of about 300 further lines, providing information on 126 new energy levels. We note that this method also implicitly provides the vibrational quantum numbers for the newly assigned levels. As a result 2030 lines out of the observed 2417 lines from the experimental line list, i.e. almost 84%, are assigned. When blends are considered, the total number of assigned lines is 2937. Some of the unassigned lines may be attributable to other species present in the flame, such as CO or CO<sub>2</sub>. For example the spectrum covers the region of the CO second overtone. However, attempts to model CO and CO<sub>2</sub> lines in this region did not produce clear matches.

Fig. 4 shows 10 cm<sup>-1</sup> of the measured spectrum around 6435 cm<sup>-1</sup> compared to the calculated line list and illustrates situations when multiple lines are associated with a single observed feature. For example, the strong, broad feature at 6432.6 cm<sup>-1</sup> consists of at least three actual transitions, however in the experimental line list these transitions are represented by a single line at the strongest peak at 6432.595 cm<sup>-1</sup>. We assigned 3 MARVEL lines to this feature; these lines have a summed intensity about 65% of the measured integral intensity of the feature, meaning it could be hiding further lines. The line at 6439.858 cm<sup>-1</sup> appears to be isolated but in fact has a double assignment with the difference between the two MARVEL frequencies of 0.05 cm<sup>-1</sup>; these lines model essentially the whole intensity of this feature. Single MARVEL assignment means that any other nearby lines are at least about an order-of-magnitude weaker.

The calculated line list contains many more weak lines than the experimental line list. These weak lines overlap with more intense

**Table 1**

Summary of vibrational bands with  $N$  lines assigned to them. Only bands for which  $N \geq 10$  are given.

band	$N$	band	$N$
021-000	187	032-011	40
101-000	182	141-120	31
200-000	142	400-200	29
120-000	75	310-110	28
002-000	36	211-011	27
011-000	27	220-001	27
040-000	10	042-021	23
111-010	93	022-100	20
301-200	68	121-001	19
102-100	65	103-002	19
211-110	65	301-101	19
102-001	64	140-020	18
400-101	56	230-011	17
310-011	55	410-111	17
210-010	49	221-120	15
061-040	46	221-200	15
131-110	43	021-010	13
022-001	42	220-100	12
130-010	41	311-210	12
121-100	40	220-020	11

water lines and therefore cannot be identified from the experimental spectrum. However, the contribution of these weak lines does not explain many apparent line strength discrepancies between the two line lists. The task of predicting line intensities for water using *ab initio* procedures is under constant review [48] and work is currently in progress at UCL to further improve the water dipole surface. Progress on this will be reported elsewhere.

A full list of the experimental lines with assignments are given in the supplementary data. This list specifies whether the line was trivially assigned using MARVEL or is associated with a new energy level. We note that the short spectral range and density of lines meant that these new energy levels are not generally confirmed by combination differences.

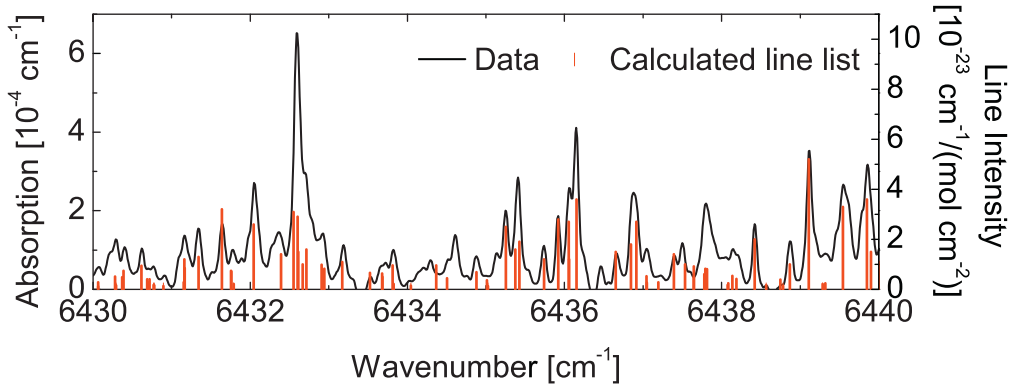


**Fig. 4.** Comparison of the measured spectrum (black, left axis) and a stick spectrum of the assigned calculated lines (red, right axis) for a small frequency window. (For interpretation of the references to colour in this figure legend, the reader is referred to the web version of this article.)

**Table 2**

Newly determined energy levels for  $\text{H}_2^{16}\text{O}$ . Observed – calculated (o-c) values, in  $\text{cm}^{-1}$ , are relative to POKAZATEL line list.

$J\text{K}_a\text{K}_c$	$v_1v_2v_3$	$E / \text{cm}^{-1}$	o-c	$J\text{K}_a\text{K}_c$	$v_1v_2v_3$	$E / \text{cm}^{-1}$	o-c	$J\text{K}_a\text{K}_c$	$v_1v_2v_3$	$E / \text{cm}^{-1}$	o-c
14 1 13	061	15,196.170	-0.044	8 3 5	061	13,975.084	-0.021	16 7 9	201	14,398.683	-0.037
15 12 3	002	11,944.059	-0.038	9 3 7	061	14,184.268	-0.033	17 0 17	201	13,436.679	-0.104
19 9 10	002	12,947.908	-0.044	6 2 4	071	14,768.262	-0.013	18 4 14	201	14,817.74	-0.064
8 1 8	004	15,233.158	-0.02	15 9 6	101	11,077.237	-0.145	18 7 11	201	15,211.965	-0.168
16 2 15	021	9813.798	-0.028	17 8 9	101	11,645.203	-0.068	10 9 2	210	11,277.802	-0.033
16 2 15	022	13,412.179	-0.057	18 9 10	101	12,258.106	-0.048	11 11 0	210	11,991.199	0.063
9 4 6	031	9852.648	-0.099	23 5 19	101	13,720.971	-0.034	12 9 4	210	11,831.292	-0.027
12 5 7	031	10,861.193	0.169	26 6 20	101	15,782.146	-0.074	12 10 3	210	12,013.462	0.018
19 7 13	031	13,925.583	-0.04	15 6 9	102	14,189.387	-0.084	12 12 1	210	12,543.449	0.067
13 7 6	032	15,168.281	-0.035	14 8 7	111	12,198.087	-0.113	13 10 3	210	12,320.932	0.011
12 10 3	040	10,359.146	-0.046	15 8 7	111	12,549.411	-0.138	13 11 2	210	12,587.499	0.035
11 5 6	041	12,161.521	0.007	16 8 9	111	12,922.244	-0.065	13 12 1	210	12,854.881	-0.059
11 6 6	041	12,401.372	-0.056	20 6 14	111	14,382.203	-0.028	15 5 10	210	12,071.533	-0.053
12 5 7	041	12,442.132	-0.024	21 8 14	111	15,088.616	-0.031	16 4 13	210	12,132.162	-0.06
12 8 4	041	13,250.26	0.007	13 4 9	112	14,878.042	0.042	17 4 13	210	12,698.242	-0.004
13 7 7	041	13,263.805	-0.121	16 9 8	120	11,396.542	-0.012	17 5 12	210	12,867.315	-0.027
14 7 7	041	13,594.493	-0.036	20 8 13	120	12,913.391	0.015	18 2 17	210	12,287.241	-0.051
16 2 14	041	13,214.275	0.081	17 3 15	121	13,851.555	-0.026	18 3 16	210	12,598.021	-0.041
19 3 17	041	14,350.205	-0.006	19 2 18	121	14,244.954	0.012	18 4 15	210	12,871.799	-0.078
5 3 3	051	11,980.727	-0.009	20 1 19	121	14,622.29	-0.126	19 1 18	210	12,646.72	-0.057
6 3 3	051	12,129.054	0.0	9 8 1	130	10,759.505	-0.006	19 2 17	210	12,974.57	-0.05
6 4 2	051	12,366.269	-0.082	10 8 3	130	11,001.243	-0.029	19 3 16	210	13,264.616	-0.067
7 2 5	051	12,135.336	-0.024	10 9 2	130	11,185.909	0.003	20 1 20	210	12,624.253	-0.056
7 5 3	051	12,805.967	-0.004	11 8 3	130	11,265.526	-0.018	20 2 19	210	13,022.745	-0.067
8 1 8	051	11,996.135	0.018	12 8 5	130	11,551.968	-0.016	21 0 21	210	12,996.448	-0.028
8 4 4	051	12,730.885	-0.023	12 9 4	130	11,736.443	-0.006	21 1 20	210	13,415.475	-0.061
9 0 9	051	12,164.81	-0.022	13 8 5	130	11,860.261	-0.03	16 9 7	211	16,439.527	-0.053
9 5 5	051	13,215.983	-0.035	13 9 4	130	12,044.351	-0.024	13 4 9	220	12,824.952	-0.043
11 2 10	051	12,914.709	-0.02	14 6 9	130	11,643.342	-0.05	10 9 2	300	12,856.023	0.029
11 7 5	051	14,302.282	0.044	14 8 7	130	12,189.994	-0.019	13 8 5	300	13,510.443	-0.045
12 1 11	051	13,157.177	0.015	12 2 11	140	11,582.593	-0.011	15 3 12	300	13,515.85	-0.053
12 7 5	051	14,586.049	-0.016	11 3 9	141	15,061.568	-0.033	16 2 15	300	13,390.283	0.132
13 3 11	051	13,756.382	-0.046	12 11 1	200	10,531.411	-0.094	16 4 13	300	13,856.623	-0.069
2 0 2	061	12,656.003	-0.004	15 9 6	200	11,086.936	-0.033	16 4 13	300	13,856.632	-0.059
2 2 0	061	12,923.888	0.007	16 6 10	200	10,935.016	-0.037	16 5 12	300	14,057.023	-0.068
3 1 3	061	12,787.646	0.035	16 10 6	200	11,651.177	-0.035	18 3 15	300	14,581.009	-0.093
3 3 1	061	13,245.215	0.01	16 13 4	200	12,398.076	0.03	18 7 12	300	15,158.842	-0.051
4 0 4	061	12,813.251	-0.015	18 5 13	200	11,650.563	-0.006	19 5 14	300	15,399.793	-0.111
4 1 3	061	12,933.841	-0.036	18 9 10	200	12,267.551	0.049	12 10 3	310	15,298.892	-0.026
4 2 2	061	13,095.518	0.001	13 4 9	201	13,052.721	-0.041	14 3 12	310	14,588.529	-0.015
4 3 2	061	13,342.05	-0.009	15 7 9	201	14,005.593	-0.075	17 3 14	310	15,807.947	-0.034

The spectrum contains transitions from 136 bands, of which 45 contain only a single transition. Table 1 shows a summary of the main bands observed in this spectrum. Only about 20% of the observed lines involve transitions from the vibrational ground state with most corresponding to hot bands. Transitions involve a large number of rotational states with  $J$  up to 27.

Table 2 presents our newly determined energy levels. Differences between these and the values predicted by the POKAZA-

TEL line list are also given. The small value of these differences and their smooth behaviour within a given vibrational state lends confidence to our new assignments. Note that these energy levels are derived from measurements made at atmospheric pressure and therefore will include small contributions due to the pressure shift. For comparison, Zobov et al. [15] analyzed a hot emission spectrum recorded using an oxy-acetylene welding torch and a Fourier transform spectrometer. In the 6250 – 6670  $\text{cm}^{-1}$  region consid-

ered here that spectrum contains a similar number of lines to the current one, albeit line positions were only determined to about  $0.02\text{ cm}^{-1}$ . Zobov et al. give 840 line assignments in this region which can be compared with 2937 here. This means that more than 70% of the line assignments given here are actually new.

## 6. Conclusion

A near-infrared absorption spectrum of water recorded in a flame at 1950 K using cavity-enhanced optical frequency comb-based Fourier transform spectrometer is shown to be a rich source of information on water transitions. About 85% of the lines observed in the spectral region  $6250\text{--}6670\text{ cm}^{-1}$  are assigned using both previous information on empirical energy levels and by comparison with a new, variational line list. Many of the experimental lines are assigned to multiple transitions. The majority of the assigned lines are actually associated with hot bands. These new data will form part of the input for the update of MARVEL energy levels for  $\text{H}_2^{16}\text{O}$ , which is currently in progress [30].

## Acknowledgements

This work was supported by NERC under various grants (NE/F01967X/1, NE/J010316/1, NE/N001508/1). A.F. acknowledges support from the Swedish Research Council (2016-03593), the Knut and Alice Wallenberg Foundation (2015.0159), and the Swedish Foundation for Strategic Research (ICA12-0031). F.M.S. acknowledges financial support by the Swedish Energy Agency (36160-1), the Kempe Foundations (JCK-1316) and the Swedish strategic research program Bio4Energy. A.A.K and N.F.Z. acknowledge support by State Project IAP RAS No. 0035-2014-009.

## References

- [1] Pine AS, Coulombe MJ, Camy-Peyret C, Flaud J-M. Atlas of the high-temperature water vapor spectrum in the  $3000\text{--}4000\text{ cm}^{-1}$  region. *J Phys Chem Ref Data* 1983;12:413–65.
- [2] Pearson JC, Anderson T, Herbst E, De Lucia FC, Helminger P. Millimeter- and submillimeter-wave spectrum of highly excited states of water. *Astrophys J* 1991;379:L41–3.
- [3] Polyansky OL, Zobov NF, Tennyson J, Lotoski JA, Bernath PF. Hot bands of water in the  $v_2$  manifold up to  $5v_2 - 4v_2$ . *J Mol Spectrosc* 1997;184:35–50.
- [4] Polyansky OL, Zobov NF, Viti S, Tennyson J, Bernath PF, Wallace L. K band spectrum of water in sunspots. *Astrophys J* 1997;489:L205–8.
- [5] Polyansky OL, Tennyson J, Bernath PF. The spectrum of hot water: rotational transitions and difference bands in the (020), (100) and (001). *J Mol Spectrosc* 1997;186:213–21.
- [6] Polyansky OL, Zobov NF, Viti S, Tennyson J, Bernath PF, Wallace L. High temperature rotational transitions of water in sunspot and laboratory spectra. *J Mol Spectrosc* 1997;186:422–47.
- [7] Esplin MP, Wattson RB, Hoke LB, Rothman LS. High-temperature spectrum of  $\text{H}_2\text{O}$  in the  $720\text{--}1400\text{ cm}^{-1}$  region. *J Quant Spectrosc Radiat Transf* 1998;60:711–39.
- [8] Zobov NF, Polyansky OL, Tennyson J, Lotoski JA, Colarusso P, Zhang K-Q, et al. Hot bands of water up to  $6v_2 - 5v_2$  in the  $933\text{--}2500\text{ cm}^{-1}$  region. *J Mol Spectrosc* 1999;193:118–36.
- [9] Zobov NF, Polyansky OL, Tennyson J, Shirin SV, Nassar R, Hirao T, et al. Using laboratory spectroscopy to identify lines in the K and L-band spectrum of water in a sunspot. *Astrophys J* 2000;530:994–8.
- [10] Tereszchuk K, Bernath PF, Zobov NF, Shirin SV, Polyansky OL, Libeskind NI, et al. Laboratory spectroscopy of hot water near 2-microns and sunspot spectroscopy in the H-band region. *Astrophys J* 2002;577:496–500.
- [11] Couder LH, Pirali O, Vervloet M, Lanquetin R, Camy-Peyret C. The eight first vibrational states of the water molecule: measurements and analysis. *J Mol Spectrosc* 2004;228:471–98.
- [12] Coheur P-F, Bernath PF, Carleer M, Colin R, Polyansky OL, Zobov NF, et al. 3200 K laboratory emission spectrum of water. *J Chem Phys* 2005;122:074307.
- [13] Zobov NF, Shirin SV, Polyansky OL, Tennyson J, Coheur P-F, Bernath PF, et al. Monodromy in the water molecules. *Chem Phys Lett* 2005;414:193–7.
- [14] Zobov NF, Shirin SV, Polyansky OL, Barber RJ, Tennyson J, Coheur P-F, et al. Spectrum of hot water in the  $2000\text{--}4750\text{ cm}^{-1}$  frequency range. *J Mol Spectrosc* 2006;237:115–22.
- [15] Zobov NF, Shirin SV, Ovsyannikov RI, Polyansky OL, Barber RJ, Tennyson J, et al. Spectrum of hot water in the  $4750\text{--}13000\text{ cm}^{-1}$  frequency range ( $0.769\text{--}2.1\mu\text{m}$ ). *Mon Not R Astron Soc* 2008;387:1093–8.
- [16] Yu S, Pearson JC, Drouin BJ, Martin-Drumel M-A, Pirali O, Vervloet M, et al. Measurement and analysis of new terahertz and far-infrared spectra of high temperature water. *J Mol Spectrosc* 2012;279:16–25.
- [17] Couder LH, Martin-Drumel M-A, Pirali O. Analysis of the high-resolution water spectrum up to the second triad and to  $J = 30$ . *J Mol Spectrosc* 2014;303:36–41. doi:[10.1016/j.jms.2014.07.003](https://doi.org/10.1016/j.jms.2014.07.003).
- [18] Allard F, Hauschildt PH, Miller S, Tennyson J. The influence of  $\text{H}_2\text{O}$  line blanketing on the spectra of cool dwarf stars. *Astrophys J* 1994;426:L39–41.
- [19] Wattson RB, Rothman LS. Direct numerical diagonalization - wave of the future. *J Quant Spectrosc Radiat Transf* 1992;48:763–80. doi:[10.1016/0022-4073\(92\)90140-Y](https://doi.org/10.1016/0022-4073(92)90140-Y).
- [20] Viti S, Tennyson J, Polyansky OL. A spectroscopic linelist for hot water. *Mon Not R Astron Soc* 1997;287:79–86.
- [21] Partridge H, Schwenke DW. The determination of an accurate isotope dependent potential energy surface for water from extensive ab initio calculations and experimental data. *J Chem Phys* 1997;106:4618–39. doi:[10.1063/1.473987](https://doi.org/10.1063/1.473987).
- [22] Jørgensen UG, Jensen P, Sorensen GO, Aringer B.  $\text{H}_2\text{O}$  in stellar atmospheres. *Astron Astrophys* 2001;372:249–59.
- [23] Barber RJ, Tennyson J, Harris GJ, Tolchenov RN. A high accuracy computed water line list. *Mon Not R Astron Soc* 2006;368:1087–94.
- [24] Polyansky OL, Kyuberis AA, Lodi L, Tennyson J, Ovsyannikov RI, Zobov N, et al. Exomol molecular line lists XXVI: a complete high-accuracy line list for water. *Mon Not R Astron Soc*. 2018 (submitted).
- [25] Rothman LS, Gordon IE, Barber RJ, Dothe H, Gamache RR, Goldman A, et al. HITRAN, the high-temperature molecular spectroscopic database. *J Quant Spectrosc Radiat Transf* 2010;111:2139–50.
- [26] Tennyson J, Yurchenko SN. Exomol: molecular line lists for exoplanet and other atmospheres. *Mon Not R Astron Soc* 2012;425:21–33. doi:[10.1111/j.1365-2966.2012.21440.x](https://doi.org/10.1111/j.1365-2966.2012.21440.x).
- [27] Tennyson J, Yurchenko SN, Al-Refaei AF, Barton EJ, Chubb KL, Coles PA, et al. The exomol database: molecular line lists for exoplanet and other hot atmospheres. *J Mol Spectrosc* 2016;327:73–94. doi:[10.1016/j.jms.2016.05.002](https://doi.org/10.1016/j.jms.2016.05.002).
- [28] Tennyson J, Bernath PF, Brown LR, Campargue A, Carleer MR, Császár AG, et al. IUPAC critical evaluation of the rotational-vibrational spectra of water vapor. Part III. Energy levels and transition wavenumbers for  $\text{H}_2^{16}\text{O}$ . *J Quant Spectrosc Radiat Transf* 2013;117:29–80. doi:[10.1016/j.jqsrt.2012.10.002](https://doi.org/10.1016/j.jqsrt.2012.10.002).
- [29] Tennyson J, Bernath PF, Brown LR, Campargue A, Császár AG, Daumont L, et al. A database of water transitions from experiment and theory (IUPAC technical report). *Pure Appl Chem* 2014;86:71–83. doi:[10.1515/pac-2014-5012](https://doi.org/10.1515/pac-2014-5012).
- [30] Furtenbacher T, Dénes N, Tennyson J, Naumenko OV, Polyansky OL, Zobov NF, et al. The 2016 update of the IUPAC database of water energy levels. *J Quant Spectrosc Radiat Transf* (in preparation).
- [31] Flaud J-M, Camy-Peyret C, Maillard J. Higher ro-vibrational levels of  $\text{H}_2\text{O}$  deduced from high resolution oxygen-hydrogen flame spectra between  $2800\text{--}6200\text{ cm}^{-1}$ . *Mol Phys* 1976;32:499–521. doi:[10.1080/0026897760103251](https://doi.org/10.1080/0026897760103251).
- [32] Camy-Peyret C, Flaud J-M, Maillard J, Guelachvili G. Higher ro-vibrational levels of  $\text{H}_2\text{O}$  deduced from high resolution oxygen-hydrogen flame spectra between  $6200$  and  $9100\text{ cm}^{-1}$ . *Mol Phys* 1977;33:1641–50. doi:[10.1080/00268977700101361](https://doi.org/10.1080/00268977700101361).
- [33] Mandin JY, Dana V, Camy-Peyret C, Flaud J-M. Collisional widths of pure rotational transitions of  $\text{H}_2\text{O}$  from fourier-transform flame spectra. *J Mol Spectrosc* 1992;152:179–84.
- [34] Dana V, Mandin JY, Camy-Peyret C, Flaud J-M, Rothman LS. Rotational and vibrational dependences of collisional linewidths in the  $n\nu_2 - (n-1)\nu_2$  hot bands of  $\text{H}_2\text{O}$  from Fourier-transform flame spectra. *Appl Opt* 1992;31:1179–1184.
- [35] Mikhailenko SN, Tyuterev VG, Starikov VI, Albert KK, Winnewisser BP, Winnewisser M, et al. Water spectra in the region  $4200\text{--}6250\text{ cm}^{-1}$ : extended analysis of  $v_1 + v_2$ ,  $v_2 + v_3$ , and  $3v_2$  bands and confirmation of highly excited states from flame spectra and from atmospheric long-path observations. *J Mol Spectrosc* 2002;213:91–121.
- [36] Alrahman C Abd, Khodabakhsh A, Schmidt FM, Qu Z, Foltynowicz A. Cavity-enhanced optical frequency comb spectroscopy of high-temperature  $\text{H}_2\text{O}$  in a flame. *Optics Express* 2014;22:13889–95.
- [37] Maslowski P, Lee KF, Johansson AC, Khodabakhsh A, Kowzan G, Rutkowski L, et al. Surpassing the path-limited resolution of fourier-transform spectrometry with frequency combs. *Phys Rev A* 2016;93:021802.
- [38] Rutkowski L, Maslowski P, Johansson AC, Khodabakhsh A, Foltynowicz A. Optical frequency comb fourier transform spectroscopy with sub-nominal resolution. *J Quant Spectrosc Radiat Transf* 2017;204:63.
- [39] Foltynowicz A, Ban T, Maslowski P, Adler F, Ye J. Quantum-noise-limited optical frequency comb spectroscopy. *Phys Rev Lett* 2011;107:233002.
- [40] Qu Z, Ghorbani R, Valiev D, Schmidt FM. Calibration-free scanned wavelength modulation spectroscopy-application to  $\text{H}_2\text{O}$  and temperature sensing in flames. *Opt Express* 2015;23:16492–9.
- [41] Rutkowski L, Johansson AC, Valiev D, Khodabakhsh A, Tkacz A, Schmidt FM, et al. Detection of OH in an atmospheric flame at  $1.5\mu\text{m}$  using optical frequency comb spectroscopy. *Photonics Lett Pol* 2016;8:110–12.
- [42] Foltynowicz A, Maslowski P, Fleisher AJ, Bjork BJ, Ye J. Cavity-enhanced optical frequency comb spectroscopy in the mid-infrared – application to trace detection of hydrogen peroxide. *Appl Phys B* 2013;110:163–75.
- [43] Hartung G, Hult J, Kaminski CF. A flat flame burner for the calibration of laser thermometry techniques. *Meas Sci Tech* 2006;17:2485–93.
- [44] Rothman LS, Gordon IE, Babikov Y, Baribe A, Benner DC, Bernath PF, et al. The HITRAN 2012 molecular spectroscopic database. *J Quant Spectrosc Radiat Transf* 2013;130:4–50. doi:[10.1016/j.jqsrt.2013.07.002](https://doi.org/10.1016/j.jqsrt.2013.07.002).

- [45] Furtenbacher T, Császár AG, Tennyson J. MARVEL: measured active rotation-al-vibrational energy levels. *J Mol Spectrosc* 2007;245:115–25.
- [46] Furtenbacher T, Császár AG. MARVEL: measured active rotational-vibrational energy levels. II. algorithmic improvements. *J Quant Spectrosc Radiat Transf* 2012;113:929–35.
- [47] Barton EJ, Yurchenko SN, Tennyson J, Béguier S, Campargue A. A near infrared line list for NH<sub>3</sub>: analysis of a kitt peak spectrum after 35 years. *J Mol Spectrosc* 2016;325:7–12. doi:[10.1016/j.jms.2016.05.001](https://doi.org/10.1016/j.jms.2016.05.001).
- [48] Birk M, Wagner G, Loos J, Lodi L, Polyansky OL, Kyuberis AA, et al. Accurate line intensities for water transitions in the infrared: comparison of theory and experiment. *J Quant Spectrosc Radiat Transf* 2017;203:88–102. doi:[10.1016/j.jqsrt.2017.03.040](https://doi.org/10.1016/j.jqsrt.2017.03.040).